A metabolic switch in proteasome inhibitor-resistant multiple myeloma ensures higher mitochondrial metabolism, protein folding and sphingomyelin synthesis

Lenka Besse,[1#] Andrej Besse,[1#] Max Mendez-Lopez,[1] Katerina Vasickova,[2] Miroslava Sedlackova,[2] Petr Vanhara,[2] Marianne Kraus,[1] Jürgen Bader,[1] Renan B. Ferreira,[3] Ronald K. Castellano,[3,4] Brian K. Law[4,5] and Christoph Driessen[1]

[#]LB and AB contributed equally to this work.

[1]Experimental Oncology and Hematology, Department of Oncology and Hematology, St. Gallen Cantonal Hospital, St. Gallen, Switzerland; [2]Department of Histology and Embryology, Faculty of Medicine, Masaryk University, Brno, Czech Republic; [3]Department of Chemistry, University of Florida, Gainesville, FL, USA; [4]UF-Health Cancer Center, University of Florida, Gainesville, FL, USA and [5]Department of Pharmacology & Therapeutics, University of Florida, Gainesville, FL, USA

Correspondence: LENKA BESSE - Lenka.besse@kssg.ch
doi:10.3324/haematol.2018.207704

SUPPLEMENTAL DATA

A metabolic switch in proteasome inhibitor resistant multiple myeloma ensures higher mitochondrial metabolism, protein folding and sphingomyelin synthesis

Lenka Besse, Andrej Besse, Max Mendez-Lopez, Katerina Vasickova, Miroslava Sedlackova, Petr Vanhara, Marianne Kraus, Jürgen Bader, Renan B. Ferreira, Ronald K. Castellano, Brian K. Law, Christoph Driessen

SUPPLEMENTAL METHODS

MASS-SPECTROMETRY METABOLITE PROFILING

Sample Preparation

All cell lines were cultured without PI for 2 weeks in 5 individual flasks/polyclonal cell line and single-cell derived cell line. Prior to collection, cells were seeded as $1x10^7$ in T75 flask, 24h after the cells were collected from a total of 30 flasks and cell pellets were snap frozen in liquid nitrogen. Frozen dry pellet was stored in -80^{o}C until processed.

Samples were prepared using the automated MicroLab STAR® system (Hamilton Company, Reno, Nevada, USA). Several recovery standards were added prior to the first step in the extraction process for QC purposes. To remove protein, dissociate small molecules bound to protein or trapped in the precipitated protein matrix, and to recover chemically diverse metabolites, proteins were precipitated with methanol under vigorous shaking for 2 min (Geno Grinder 2000; Glen Mills, Clifton, NJ, USA) followed by centrifugation. The resulting extract was divided into five fractions: two for analysis by two separate reverse phase (RP)/UPLC-MS/MS methods with positive ion mode electrospray ionization (ESI), one for analysis by RP/UPLC-MS/MS with negative ion mode ESI, one for analysis by HILIC/UPLC-MS/MS with negative ion mode ESI, and one sample was reserved for backup. Samples were placed briefly on a TurboVap® (Zymark, SOTAX, Switzerland) to remove the organic solvent. The sample extracts were stored overnight under nitrogen before preparation for analysis.

Ultrahigh Performance Liquid Chromatography-Tandem Mass Spectroscopy (UPLC-MS/MS)

All methods utilized a Waters ACQUITY ultra-performance liquid chromatography (UPLC) and Q-Exactive high resolution/accurate mass spectrometer (Thermo Fisher Scientific, MA; USA) interfaced with a heated electrospray ionization (HESI-II) source and Orbitrap mass analyzer operated at 35 000 mass resolution. The sample extract was dried, then reconstituted in solvents compatible to each of the four methods. Each reconstitution solvent contained a series of standards at fixed concentrations to ensure injection and chromatographic consistency. One aliquot was analyzed using acidic positive ion conditions, chromatographically optimized for more hydrophilic compounds. In this method, the extract was gradient eluted from a C18 column (Waters UPLC BEH C18-2.1x100 mm, 1.7 µm) using water and methanol, containing 0.05% perfluoropentanoic acid (PFPA) and 0.1% formic acid (FA). Another aliquot was also analyzed using acidic positive ion conditions; however, it was chromatographically optimized for more hydrophobic compounds. In this method, the extract was gradient eluted from the same afore mentioned C18 column using methanol, acetonitrile, water, 0.05% PFPA and 0.01% FA and was operated at an overall higher organic content. Another aliquot was analyzed using basic negative ion optimized conditions using a separate dedicated C18 column. The basic extracts were gradient eluted from the column using methanol and water; however, with 6.5mM Ammonium Bicarbonate at pH 8. The fourth aliquot was analyzed via negative ionization following elution from a HILIC column (Waters UPLC BEH Amide 2.1x150 mm, 1.7 µm) using a gradient consisting of water and acetonitrile with 10mM Ammonium Formate, pH 10.8. The MS analysis alternated between MS and data-dependent MS^n scans using dynamic exclusion. The scan range varied slighted between methods but covered 70-1000 m/z. Raw data files are archived and extracted as described below.

Bioinformatics

The informatics system consisted of four major components, the Laboratory Information Management System (LIMS), the data extraction and peak-identification software, data processing tools for QC and compound identification, and a collection of information interpretation and visualization tools for use by data analysts. The hardware and software foundations for these informatics components were the LAN backbone, and a database server running Oracle 10.2.0.1 Enterprise Edition.

Data Extraction and Compound Identification

Raw data was extracted, peak-identified and QC processed using Metabolon's hardware and software. Compounds were identified by comparison to library entries of purified standards or recurrent unknown entities. Metabolon maintains a library based on authenticated standards that contains the retention time/index (RI), mass to charge ratio (*m/z)*, and chromatographic data (including MS/MS spectral data) on all molecules present in the library. Furthermore, biochemical identifications are based on three criteria: retention index within a narrow RI window of the proposed identification, accurate mass match to the library +/- 10 ppm, and the MS/MS forward and reverse scores between the experimental data and authentic standards. The MS/MS scores are based on a comparison of the ions present in the experimental spectrum to the ions present in the library spectrum. While there may be similarities between these molecules based on one of these factors, the use of all three data points can be utilized to distinguish and differentiate biochemicals. More than 3300 commercially available purified standard compounds have been acquired and registered into LIMS for analysis on all platforms for determination of their analytical characteristics. Additional mass spectral entries have been created for structurally unnamed biochemicals, which have been identified by virtue of their recurrent nature (both chromatographic and mass spectral). These compounds have the potential to be identified by future acquisition of a matching purified standard or by classical structural analysis.

Metabolite Quantification and Data Normalization

Peaks were quantified using area-under-the-curve. For studies spanning multiple days, a data normalization step was performed to correct variation resulting from instrument inter-day tuning differences. Essentially, each compound was corrected in run-day blocks by registering the medians to equal one (1.00) and normalizing each data point proportionately. For studies that did not require more than one day of analysis, no normalization is necessary, other than for purposes of data visualization. In certain instances, biochemical data may have been normalized to an additional factor (e.g., cell counts, total protein as determined by Bradford assay, osmolality, etc.) to account for differences in metabolite levels due to differences in the amount of material present in each sample.

Metabolite pathway analysis

Metaboanalyst v3.0 software was used for metabolite pathway analysis and metabolite set enrichment analysis in PI-resistant cells.[1,2]

CELL LINES AND PRIMARY CELLS

Cell lines were maintained in the RPMI-1640 culture medium (Sigma Aldrich, Buchs, Switzerland) supplemented with 10% heat-inactivated fetal bovine serum (FBS), 100 µg/ml streptomycin and 100U/ml penicillin/streptomycin (Sigma Aldrich, Buchs, Switzerland). The AMO-1 and L363 PI-resistant cell lines were established and maintained from their parental cell line by continuous drug exposure > 12 months.[3] Cell lines were STR-typed to confirm the authenticity (DSMZ, Braunschweig, Germany) and routinely tested for mycoplasma contamination (MycoAlert mycoplasma detection kit, Lonza, Basel, Switzerland). Primary cells were obtained from multi-drug refractory MM patients during routine diagnostic procedures after approval by the independent cantonal ethical committee and after obtaining written informed consent form. Patients' baseline characteristics are included in Table S3.

CHEMICALS USED

For the experiments, chemical were obtained as follows: proteasome inhibitors bortezomib (LC Laboratories, Woburn, MA, USA) and carfilzomib (MedChem Express, Solentuna, Sweden), Dithiotreitol (DTT, Sigma-Aldrich Buchs, Switzerland), PDI inhibitor 16F16 (Sigma-Aldrich, Buchs, Switzerland), disulfide bond disrupting agent TCyDTDO (kind gift from Brian Law, University of Florida), BCL-2 inhibitor venetoclax (LC Laboratories, Woburn, MA, USA), AMPK inhibitor Compound C (Tocris, Minneapolis, MN, USA) sphingomyelin synthase inhibitor D609 (Sigma-Aldrich, Buchs, Switzerland) and sphingolipid metabolism inhibitor tamoxifen (Sigma-Aldrich, Buchs, Switzerland).

TCyDTDO COMPOUND SYNTHESIS

TCyDTDO, a disulfide bond disrupting agent that induces unfolded protein response,[4] was synthesized through significant modification of a published route.[5] Full synthetic and characterization details will be reported elsewhere.

VIABILITY ASSAY

For the cell lines, cell viability assay was performed by seeding 10.000 cells/well in 100 µl of growth medium in 96-well plates. Cell viability was determined after 48h by MTS tetrazolium compound using CellTiter 96® AQueous One Solution according to manufacturer's recommendations (Promega, WI, USA). IC_{50} value was determined by GraphPad Prism software v.5 (La Jolla, CA, USA) using the nonlinear regression model.

For primary cells, cell viability assay was performed by seeding 10.000 cells/well in 100 µl of DMEM medium (Gibco, ThermoFisher Scientific, CA, USA) supplemented with 20% FCS in 96-well plates. Cell viability was determined after 48h by CellTiter-Glo luminescent cell viability assay (Promega, WI, USA).

INTRACELLULAR ROS BUFFERING CAPACITY

Cells were incubated with 10µM 2′,7′-Dichlorofluorescin diacetate (H_2DCFDA; Sigma-Aldrich, Buchs, Switzerland) for 20 min at 37°C. Then, cells were exposed to 0.08% H_2O_2 for 30 min, washed and green fluorescence intensity was examined by FACS Canto II (BD Biosciences, CA, USA), data were evaluated using FlowJo v10 Software (FlowJo Company, Ashland, OR, USA).

FOLDING CAPACITY BY MERO-GFP CONSTRUCT

MERO-GFP (mammalian endoplasmic reticulum-localized redox-sensitive green fluorescent protein, a gift from Prof. Urano, Department of Medicine, Division of Endocrinology, Metabolism, and Lipid Research, Washington) construct is an ER-specific redox sensor equipped with the signal sequence of mouse BiP and the mammalian ER retention signal KDEL to the N-terminus and C-terminus of the redox-sensitive GFP, respectively, which displays distinct excitation spectra in the fully oxidized and reduced state, with maxima at 394 nm and 473 nm respectively.[6,7] The cells were equipped with the construct by lentiviral transduction. Briefly, lentivirus was produced by packaging plasmids pMD2.G and psPAX2 (a gift from Trono's lab; Addgene plasmids #12259 and #12260) and the MERO-GFP transfer plasmid in HEK-293-LentiX cell line (Clontech/Takara Bio, Saint-Germain-en-Laye, France). Virus was collected after 60 h and concentrated using Peg-it Virus precipitation solution (System Biosciences, Palo Alto, CA, USA). After transduction, the cells were selected with puromycin (Sigma-Aldrich, Buchs, Switzerland) and the respective fluorescence of folded and unfolded GFP was evaluated by BD Fortessa flow cytometer (BD Biosciences, San Jose, CA, USA) at 405 and 488 nm respectively.

ATP/ADP EVALUATION IN DIFFERENT MM CELL COMPARTMENTS

Cells were equipped with fluorescent sensors of ATP/ADP ratio targeted specifically to cytosol (GW1-Perceval HR; Addgene plasmid #49082) or to the endoplasmic reticulum (ERAT4.01; Next Generation Fluorescence Imaging GmbH, Medical University of Graz, Graz, Austria) by lentiviral transduction as described above. Afterwards, the cells were sorted

using BioRad sorter S3 (BioRad, Hercules, CA, USA) and ATP/ADP ratio was evaluated on enriched population of the cells stably expressing given construct using BD Fortessa flow cytometer (BD Biosciences, San Jose, CA, USA).

TRANSMISSION ELECTRON MICROSCOPY (TEM)

AMO-1 cells and their derivatives were washed in 0.1 M cacodylate buffer, fixed in 3% glutaraldehyde with 0.2% tannin in cacodylate buffer for 1 hour, and postfixed in 1% OsO 4 in the same buffer for 50 min. After post-fixation, cells were washed three times in cacodylate buffer and embedded in 1% agar. Agar blocks were dehydrated in increasing concentrations of ethanol (50%, 70%, 96% and 100%), treated with 100% acetone, and embedded in Durcupan resin. Ultrathin sections were prepared on Leica EM UC6 ultramicrotome, stained with uranyl acetate and Reynold´s lead citrate, and examined with FEI Morgagni 286(D) TEM. Cytological analysis of TEM images was performed by two independent reviewers (PV, MS).

GSH, NADP+ and NADPH evaluation

Total and relative levels of GSH, NADP+ and NADPH were determined by the luminescence intensity in AMO-1, AMO-BTZ and AMO-CFZ as well as in L363, L363-BTZ and L363-CFZ cells using GSH-Glo Glutathione Assay and NADP+/NADPH-Glo Assay(both Promega, WI, USA) according to manufacturer's recommendation.

STATISTICAL ANALYSIS

Statistical evaluation was performed in GraphPad Prism v.5 (La Jolla, CA, USA). For determination of the significance level, two-tailed unpaired t-test was used, values $p<0.05$ were considered as statistically significant. If not indicated otherwise, results are presented as a mean of at least 3 independent experiments. The coefficient of drug interaction (CDI) was determined as described previously.[8]

SUPPLEMENTAL FIGURES

Figure S1: Global metabolomic analysis of AMO-1 model cells. (A) Principal component analysis (PCA) and **(B)** hierarchical cluster analysis (HCA) of the populations of proteasome inhibitor (PI) adapted MM cells to bortezomib and carfilzomib (AMO-BTZ and AMO-CFZ, respectively) vs PI-sensitive cells. WT indicates PI-sensitive AMO-1 cells, whereas aBTZ indicates AMO-BTZ and aCFZ indicates AMO-CFZ cells. B indicates bulk, polyclonal culture whereas S indicates a single cell-derived population of the cells with respective number of the population. In **(A)** different colors and shapes indicate different populations that were compared. In **(B),** different colors horizontally indicate cell populations that cluster together, whereas the colors vertically indicate the pathways of metabolites that differ between the populations.

A)

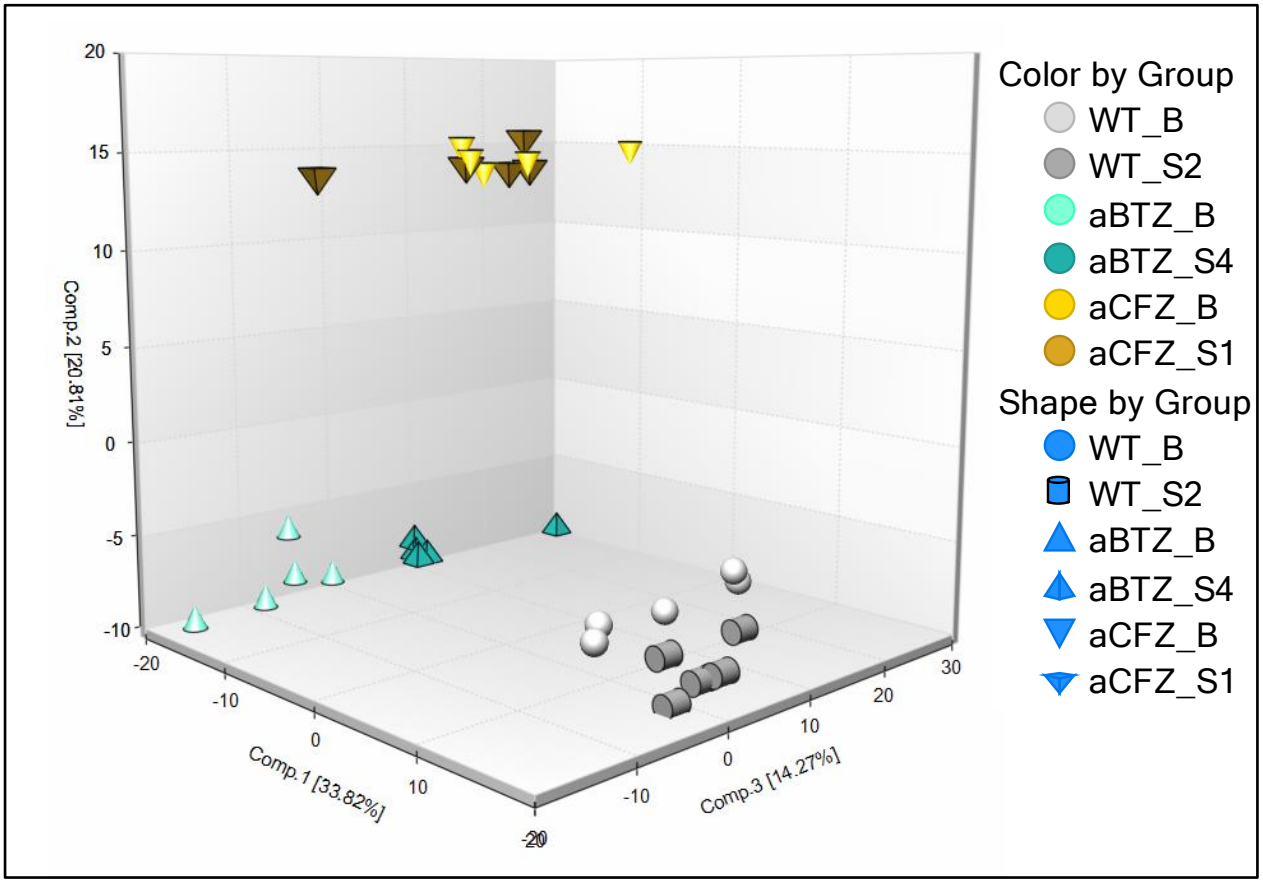

B)

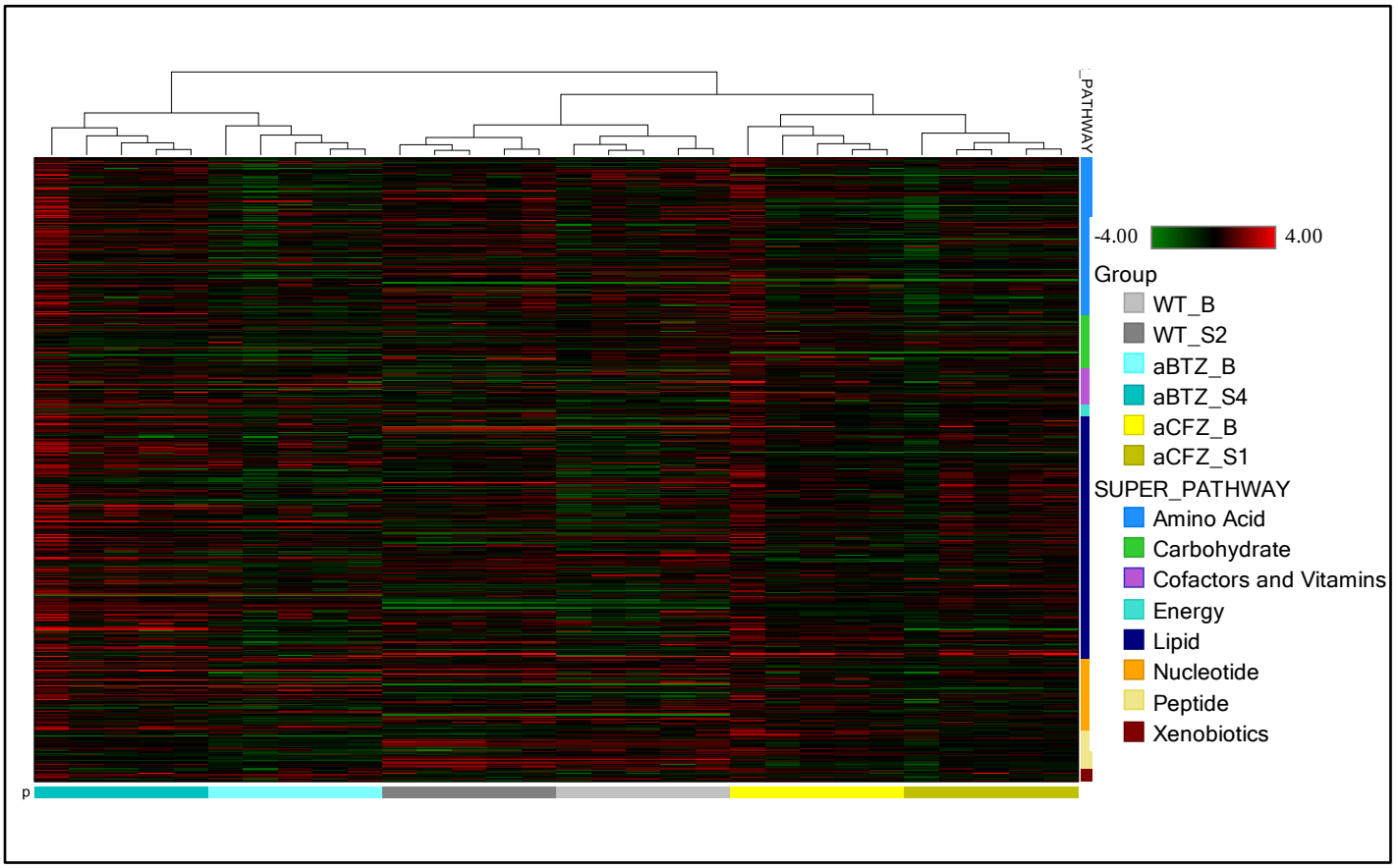
_PATHWAY
-4.00
4.00
Group
WT_B
WT_S2
aBTZ_B
aBTZ_S4
aCFZ_B
aCFZ_S1
SUPER_PATHWAY
Amino Acid
Carbohydrate
Cofactors and Vitamins
Energy
Lipid
Nucleotide
Peptide
Xenobiotics
p

Figure S2: Individual assays of GSH, NADP+ and NADPH in PI-sensitive and PI-resistant cells. Normalized level of **A)** GSH, **B)** NADP+, **C)** NADPH and **D)** NADP+/NADPH ratio evaluated by the luminescence assay in AMO-1 and L363 proteasome inhibitor sensitive (AMO-1, L363) and in bortezomib (BTZ) and carfilzomib (CFZ) resistant cells. RLU = relative luminescence units. Statistical significance is depicted with asterisks as *** $p<0.001$.

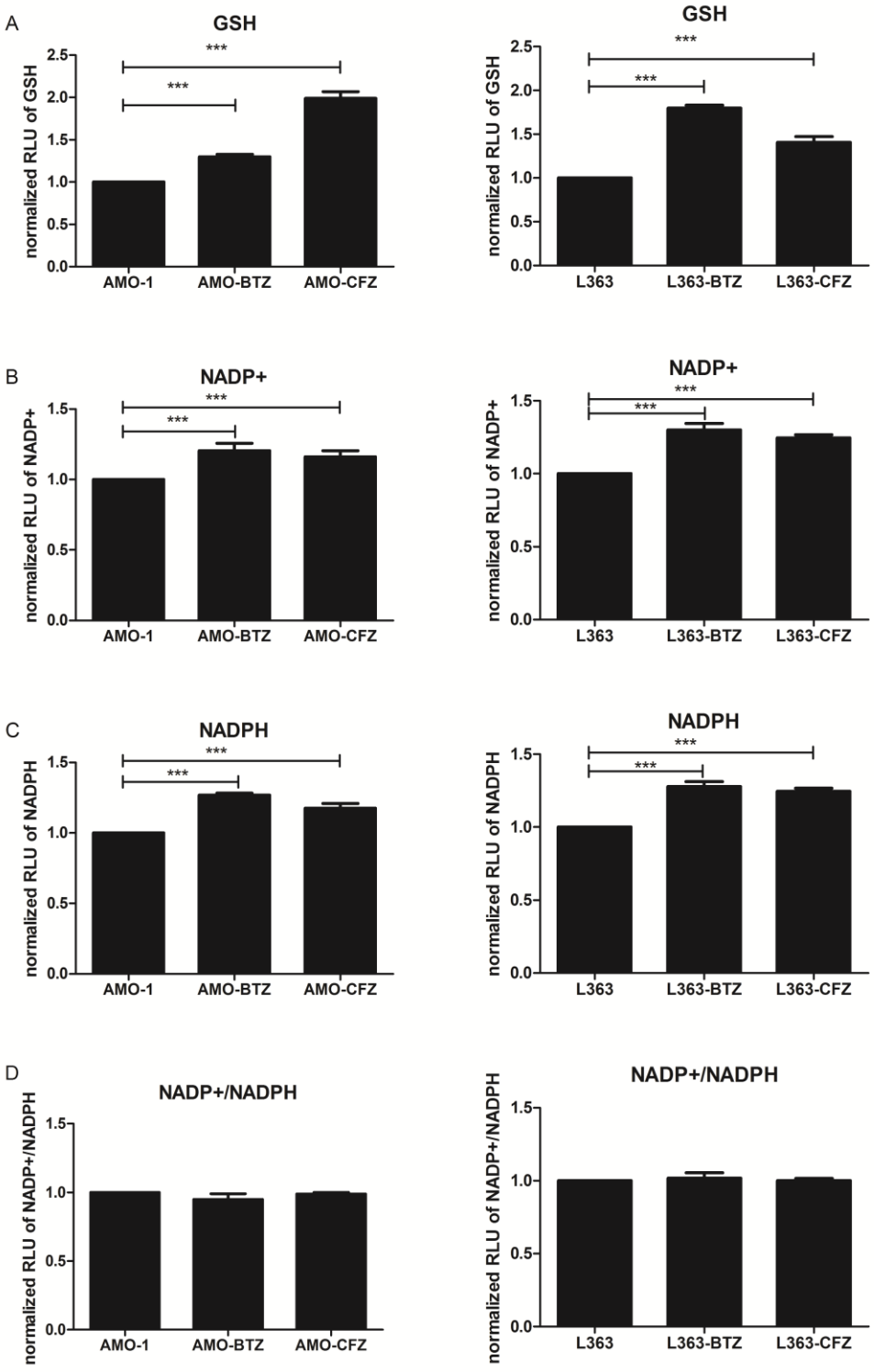

Figure S3: Metabolic shift of proteasome inhibitor (PI)-resistant cells towards increased glutathione synthesis, NAD(P)/NAD(P)H production and the TCA cycle. Schematic representation of major and consistent changes in PI-resistant cells in **(A)** glutathione synthesis pathway, containing deregulated glycine/serine, cysteine/methionine and gamma-glutamyl/glutathione metabolism; **B)** NAD(P)/NAD(P)H production, containing purine, pyrimidine, arginine/proline and alanine/aspartate/glutamate metabolism; **(C)** pantothenate pathway leading to increases level of CoA to fuel TCA cycle. These changes lead predominantly to increased antioxidant capacity and ATP production. In green are marked metabolites decreased in PI-adapted cells; in red are metabolites accumulated in PI-adapted cells.

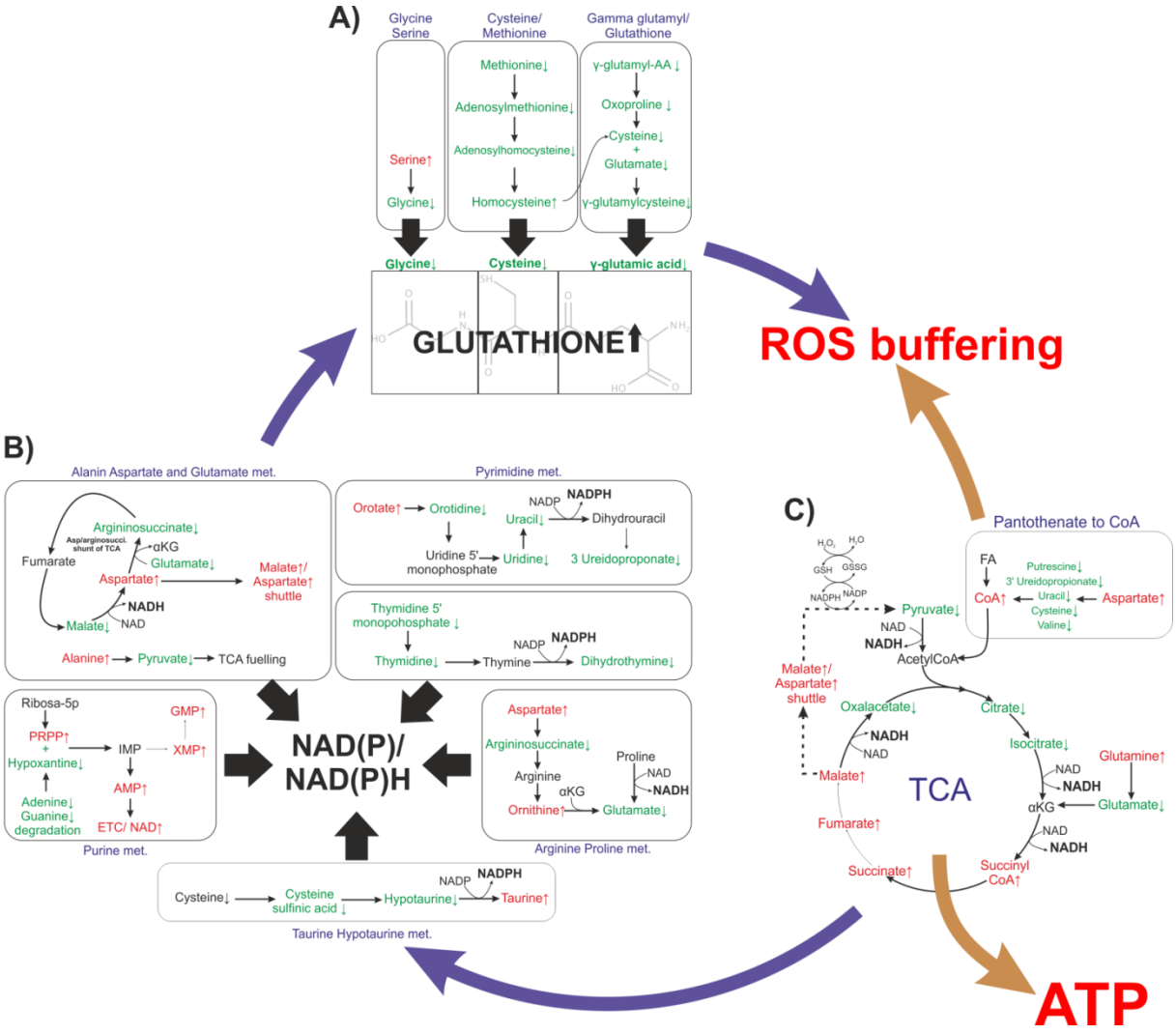

Figure S4: Dose response curves of AMO-1 sensitive, AMO-1-bortezomib resistant (AMO-BTZ) and AMO-1-carfilzomib resistant (AMO-CFZ) cells to increasing dose of H2O2. IC_{50} values are presented in Supplemental Table S2.

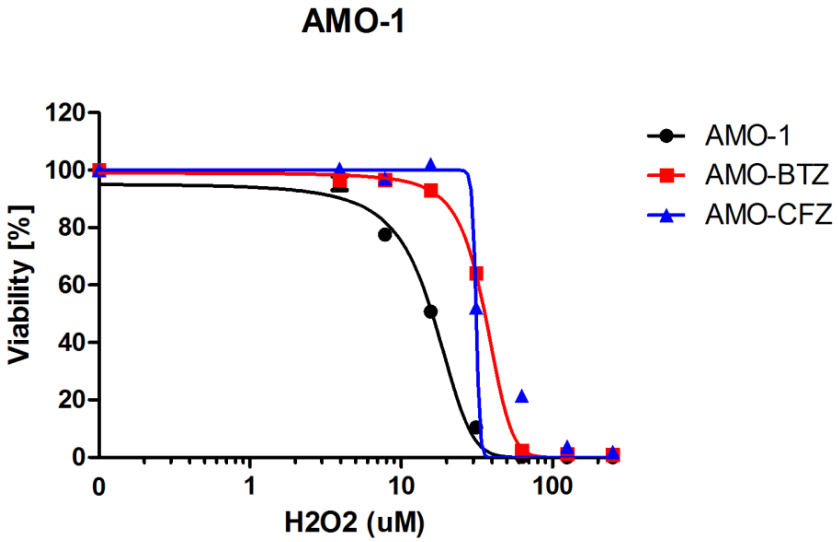

Figure S5: Viability assay of PI-sensitive AMO-1 and PI-resistant AMO-BTZ and AMO-CFZ after exposure to protein folding disruptor TCyDTDO. (A) Combination of indicated concentrations of TCyDTDO with proteasome inhibitors bortezomib (BTZ) and carfilzomib (CFZ) in AMO-BTZ (A) and AMO-CFZ (B) cells. Data represent mean ±SEM of 3 independent measurements. Statistical significance is depicted with asterisks as * $p<0.05$, ** $p<0.01$, *** $p<0.001$. **(B)** Primary malignant plasma cells were exposed for 48h to bortezomib (BTZ; MM1: 5 nM, MM2: 2.5 nM, MM3: 5 nM) and carfilzomib (CFZ; all 5 nM) alone or in combination with 0.5 µM TCyDTDO. The coefficient of drug interaction (CDI) is indicated. CDI < 1 indicates a synergistic effect; CDI = 1 indicates an additive effect; CDI > 1 indicates an antagonistic effect.

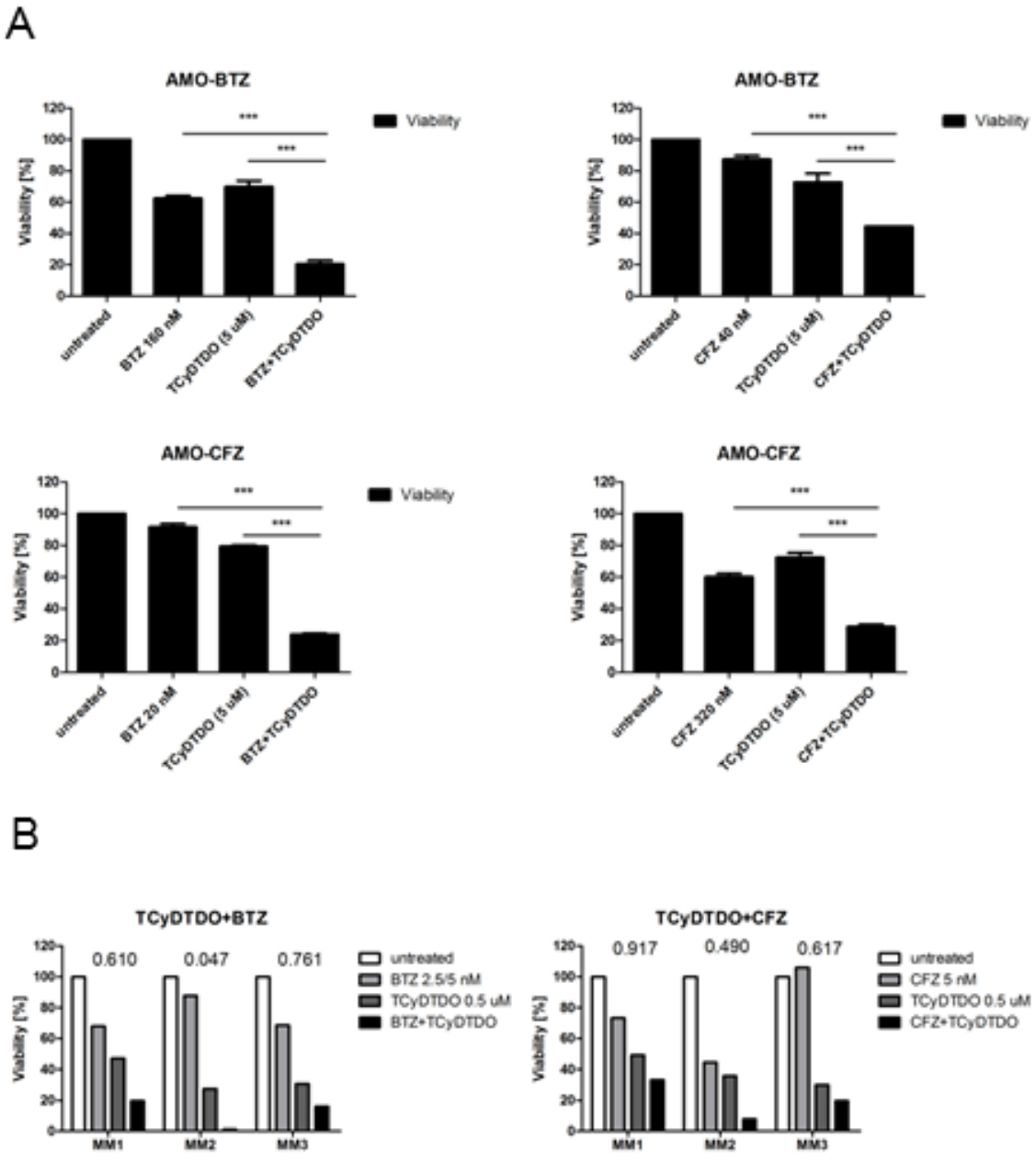

Figure S6: Viability assay of PI-sensitive and PI-resistant cell line L363 after exposure to drugs targeting mitochondria. Dose response curves of L363 sensitive, L363-bortezomib resistant (L363-BTZ) and L363-carfilzomib resistant (L363-CFZ) cells to increasing doses of BCL2 inhibitor Venetoclax and AMPK inhibitor Compound C. IC_{50} values are presented in Supplemental Table S2.

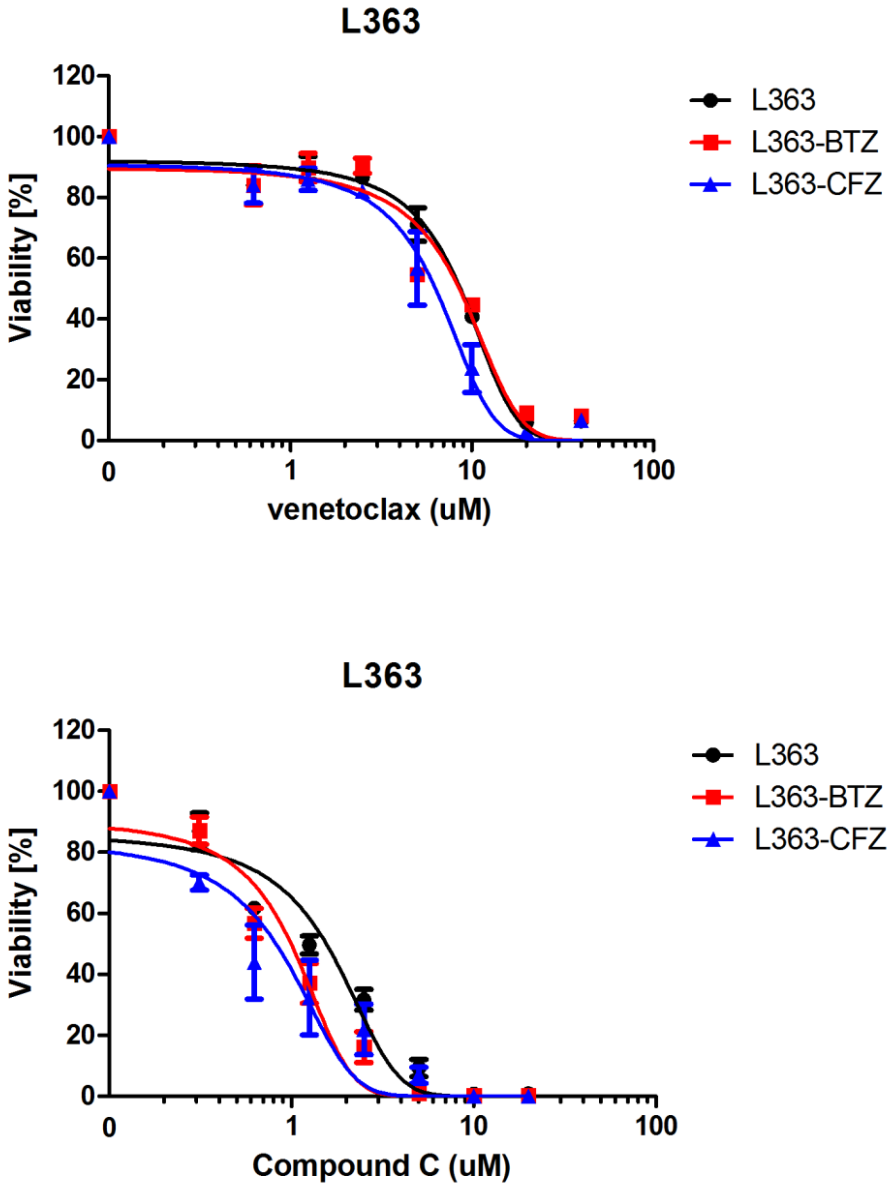

Figure S7: Overview of metabolic changes contributing to resistance to proteasome inhibitors. Proteasome inhibitor adapted cells underwent a broad metabolome shift allowing at the end more effective protein folding which confers the resistance to proteasome inhibitors. Briefly, the metabolism of carbohydrates and lipids is changed towards maximum supply of metabolic intermediates towards the TCA cycle for oxidative phosphorylation. This provides the energy supply for maximum generation of NAD(P)H, which in turn allows the recovery of GSH from GSSG that enables optimized formation of thiol bonds in newly folded protein, minimizing the proteasomal load in misfolded protein, ultimately resulting in independence from proteasome function and PI-resistance.

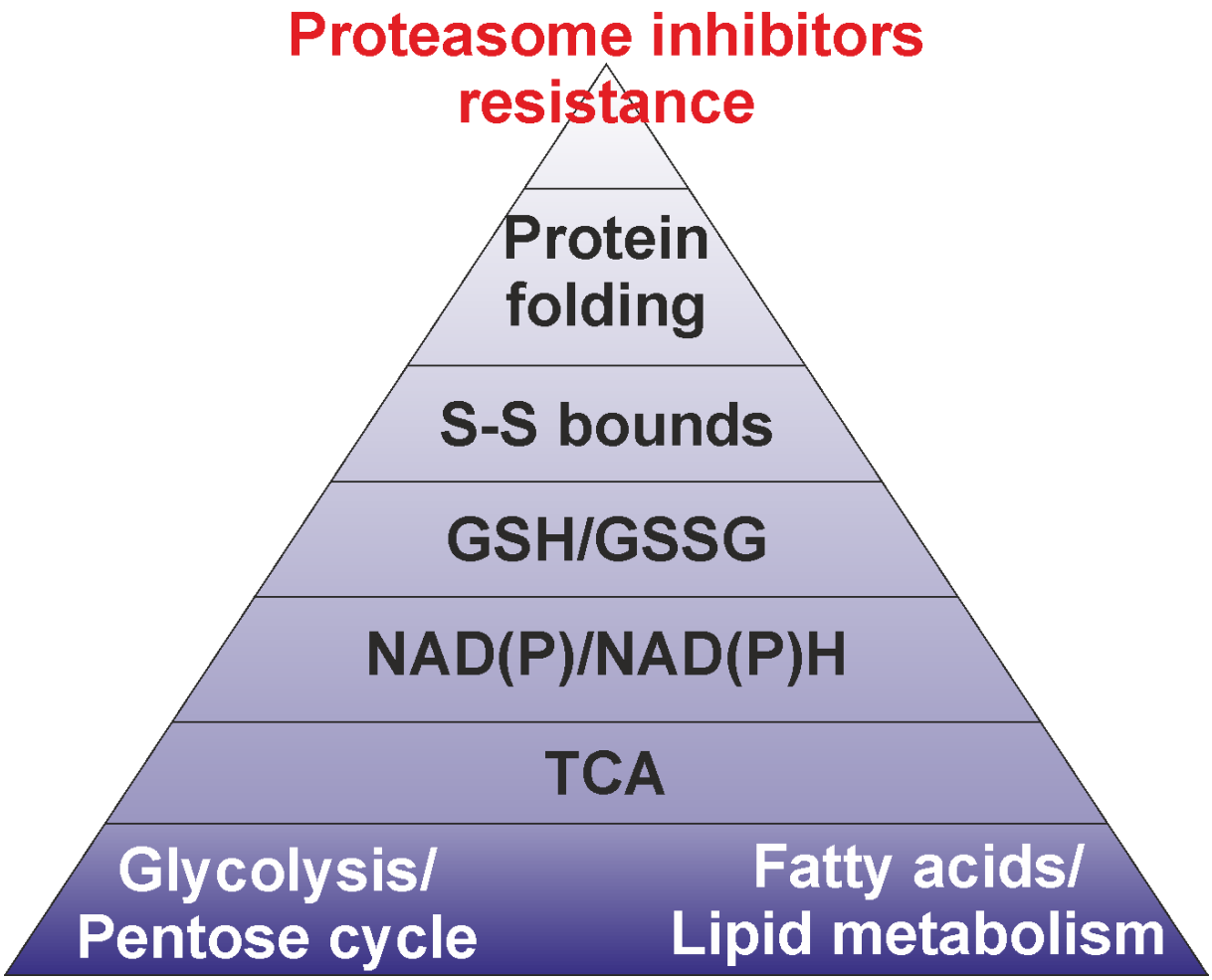

SUPPLEMENTAL TABLES

Table S1 (on separate sheet): Results of a targeted metabolomic profiling in AMO-1 cells. A summary of all biochemicals that achieved statistical significance ($p \leq 0.05$), as well as those approaching significance ($0.05 < p < 0.10$) in PI-resistant cells (aBTZ = resistant to bortezomib; aCFZ = resistant to carfilzomib) versus PI-sensitive AMO-1 (wt) cells in polyclonal culture (bulk; B) as well as in single cell derived cell populations (subclone; S with respective number of the clone).

Table S2: IC_{50} values of different chemicals used in proteasome inhibitor sensitive and resistant cells. Cytotoxicity assays with respective chemical were used to determine IC_{50} values in proteasome inhibitor (PI)-sensitive cells (AMO-1 and L363) and PI-resistant cells (AMO-BTZ; L363-BTZ = cells resistant to bortezomib; AMO-CFZ, L363-CFZ = cell resistant to carfilzomib).

IC50 values	Venetoclax (µM)	Compound C (µM)	D609 (µM)	Tamoxifen (µM)	H2O2 (µM)	BTZ (nM)	CFZ (nM)
AMO-1	7.749	2.177	2.017	1.400	16.04	2.163	1.46
AMO-BTZ	4.875	0.459	1.430	5.561	35.73	142.7	12.87
AMO-CFZ	2.850	0.954	1.747	8.125	31.33	26.82	145.7
L363	8.640	1.553	1.982	2.224	6.224	7.951	1.113
L363-BTZ	8.523	0.995	1.822	4.720	8.099	260.6	18.87
L363-CFZ	6.306	0.823	1.927	5.378	4.937	26.09	116

Table S3: Baseline characteristics of MM patients included in the study.

Patients	MM1	MM2	MM3
Age	51	74	69
Sex	F	F	F
Number of previous treatment lines	3	5	1
PCs site	Peripheral blood	Bone marrow	Peripheral blood
Previously refractory to BTZ	yes	yes	yes
Previously refractory to CFZ	yes	yes	no
Extramedullary manifestation	yes	no	yes
Primary PCL	no	no	no
Secondary PCL	yes	no	yes

Table S4: Specific changes in lipid profile of both bortezomib- and carfilzomib-resistant cells. Data are presented as a fold change of metabolite quantity between proteasome inhibitor (PI)-resistant AMO-BTZ (resistant to bortezomib) and AMO-CFZ (resistant to carfilzomib) and PI-sensitive AMO-1 cells. Fold change of **A)** representative sphingolipids, phospho- and lysolipids, **B)** representative monoacylglycerols and diacylglycerols that achieved statistical significance ($p \leq 0.05$; in dark red are those upregulated in PI-resistant cells, in dark green are those downregulated in PI-resistant cells), as well as those approaching significance ($0.05 < p < 0.10$; marked in light green) in PI-resistant cells versus PI-sensitive AMO-1 cells.

A

		Comparison	
Subpathway	**Biochemical name**	**AMO-BTZ/AMO-1**	**AMO-CFZ/AMO-1**
Sphingolipids	behenoyl sphingomyelin (d18:1/22:0)*	1.56	2.25
	sphingomyelin (d18:1/22:1, d18:2/22:0, d16:1/24:1)*	3.97	2.70
	sphingomyelin (d18:1/20:0, d16:1/22:0)*	3.07	2.07
	palmitoyl dihydrosphingomyelin (d18:0/16:0)*	1.77	2.09
	sphingomyelin (d18:1/15:0, d16:1/17:0)*	2.41	1.77
	sphingomyelin (d18:1/21:0, d17:1/22:0, d16:1/23:0)*	5.22	4.52
	sphingomyelin (d18:2/23:0, d18:1/23:1, d17:1/24:1)*	2.15	2.07
	sphingomyelin (d18:2/24:1, d18:1/24:2)*	1.61	1.84
	tricosanoyl sphingomyelin (d18:1/23:0)*	2.03	2.68
Phospho and Lysolipids	2-palmitoyl-GPC (16:0)*	0.18	0.43
	1,2-dipalmitoyl-GPC (16:0/16:0)	0.81	0.54
	1,2-dioleoyl-GPG (18:1/18:1)	0.79	0.63
	1,2-dioleoyl-GPI (18:1/18:1)	0.59	0.61
	1-palmitoyl-2-stearoyl-GPC (16:0/18:0)	0.47	0.53
	1-palmitoyl-GPC (16:0)	0.23	0.60
	2-palmitoyl-GPC (16:0)*	0.18	0.43
	1-palmitoleoyl-GPC (16:1)*	0.31	0.59
	1-stearoyl-GPC (18:0)	0.27	0.58
	1-oleoyl-GPC (18:1)	0.26	0.45
	1-linoleoyl-GPC (18:2)	0.71	0.54
	1-palmitoyl-GPE (16:0)	0.38	0.85
	2-stearoyl-GPE (18:0)*	0.12	0.51
	1-oleoyl-GPE (18:1)	0.34	0.70
	1-linoleoyl-GPE (18:2)*	0.47	0.63
	1-palmitoyl-GPI (16:0)*	0.28	0.62
	1-stearoyl-GPI (18:0)	0.30	0.60
	1-oleoyl-GPI (18:1)*	0.17	0.32
	1-oleoyl-GPS (18:1)	0.43	0.56
	1-palmitoyl-GPS (16:0)*	0.39	0.67
	1-stearoyl-GPG (18:0)	0.26	0.48
	1-oleoyl-GPG (18:1)*	0.42	0.39

B

Monoacylglycerols	1-myristoylglycerol (14:0)	1.36	1.97
	2-myristoylglycerol (14:0)	1.29	2.12
	1-palmitoylglycerol (16:0)	0.90	1.45
	2-palmitoylglycerol (16:0)	0.74	1.60
	1-oleoylglycerol (18:1)	1.57	1.97
	2-oleoylglycerol (18:1)	0.96	1.75
	1-linoleoylglycerol (18:2)	2.05	2.41
	2-linoleoylglycerol (18:2)	1.92	2.56
	1-arachidonylglycerol (20:4)	2.31	2.29
	2-arachidonoylglycerol (20:4)	1.63	1.91
	1-docosahexaenoylglycerol (22:6)	2.26	1.90
	1-dihomo-linolenylglycerol (20:3)	1.36	1.02
	1-palmitoleoylglycerol (16:1)*	1.48	2.46
	2-palmitoleoylglycerol (16:1)*	1.16	2.69
Diacylglycerols	diacylglycerol (14:0/18:1, 16:0/16:1) [2]*	0.24	0.91
	palmitoyl-oleoyl-glycerol (16:0/18:1) [2]*	0.40	1.08
	palmitoleoyl-oleoyl-glycerol (16:1/18:1) [2]*	0.41	0.91
	palmitoyl-palmitoyl-glycerol (16:0/16:0) [2]*	0.34	0.79
	oleoyl-oleoyl-glycerol (18:1/18:1) [1]*	0.53	0.53
	oleoyl-oleoyl-glycerol (18:1/18:1) [2]*	0.40	0.78

REFERENCES

1. Xia J, Wishart DS. Using MetaboAnalyst 3.0 for Comprehensive Metabolomics Data Analysis. Curr Protoc Bioinformatics. 2016 Sep 07;55:14 0 1- 0 91.
2. Xia J, Wishart DS. MSEA: a web-based tool to identify biologically meaningful patterns in quantitative metabolomic data. Nucleic Acids Res. 2010 Jul;38(Web Server issue):W71-7.
3. Soriano GP, Besse L, Li N, Kraus M, Besse A, Meeuwenoord N, et al. Proteasome inhibitor-adapted myeloma cells are largely independent from proteasome activity and show complex proteomic changes, in particular in redox and energy metabolism. Leukemia. 2016 Nov;30(11):2198-207.
4. Ferreira RB, Wang M, Law ME, Davis BJ, Bartley AN, Higgins PJ, et al. Disulfide bond disrupting agents activate the unfolded protein response in EGFR- and HER2-positive breast tumor cells. Oncotarget. 2017 Apr 25;8(17):28971-89.
5. Bass SW, Evans SA. Carbon-13 nuclear magnetic resonance spectral properties of alkyl disulfides, thiolsulfinates, and thiolsulfonates. The Journal of Organic Chemistry. 1980 1980/02/01;45(4):710-5.
6. Merksamer PI, Trusina A, Papa FR. Real-time redox measurements during endoplasmic reticulum stress reveal interlinked protein folding functions. Cell. 2008 Nov 28;135(5):933-47.
7. Kanekura K, Ishigaki S, Merksamer PI, Papa FR, Urano F. Establishment of a system for monitoring endoplasmic reticulum redox state in mammalian cells. Lab Invest. 2013 Nov;93(11):1254-8.
8. Li X, Lin Z, Zhang B, Guo L, Liu S, Li H, et al. beta-elemene sensitizes hepatocellular carcinoma cells to oxaliplatin by preventing oxaliplatin-induced degradation of copper transporter 1. Sci Rep. 2016 Feb 12;6:21010.